Available online at www.sciencedirect.com
ScienceDirect
Energy Reports 7 (2021) 357–368
www.elsevier.com/locate/egyr

The 4th International Conference on Electrical Engineering and Green Energy CEEGE 2021, 10–13 June, Munich, Germany

A hybrid model of energy scheduling for integrated multi-energy microgrid with hydrogen and heat storage system

Mengge Shi[a], Han Wang[a], Cheng Lyu[a,b], Peng Xie[a], Zhao Xu[b], Youwei Jia[a,*]

[a] Department of Electrical and Electronic Engineering, Southern University of Science and Technology, Shenzhen, 518055, China
[b] Department of Electrical Engineering, The Hong Kong Polytechnic University, Hong Kong SAR, 999077, China

Received 20 July 2021; accepted 5 August 2021

Abstract

To increase the energy utilization efficiency, it becomes fairly promising to convert the surplus electricity from renewable generation to other forms of energy for multi-dimensional consumption. In this paper, we propose a hybrid energy scheduling model for a multi-energy microgrid with the integration of the hydrogen energy storage system (HESS) and the heat storage system (HSS). In our study, the operational uncertainties induced by renewables and loads (including electrical, hydrogen, and heat demand) are comprehensively considered. We investigate such an operating regime that HESS stores the surplus electricity in case of abundant renewable generation and generates electricity through hydrogen fuel cells otherwise. Further, heat units including HESS, combined heat and power (CHP), and external heat suppliers are modeled in this paper. We split the decision-makings of energy scheduling for both the day-ahead stage and real-time stage to tackle the power balancing issues. To effectively solve the aforementioned optimization model, a flexible weighted Model Predictive Control (weighted-MPC) strategy is proposed, in which the receding horizon can be suitably adjusted according to the forecasting accuracy of system uncertainties. The effectiveness of the proposed hybrid model for microgrid energy scheduling is comprehensively verified through extensive case studies.

Peer-review under responsibility of the scientific committee of the 4th International Conference on Electrical Engineering and Green Energy, CEEGE, 2021.

Keywords: Multi-energy microgrid; Energy scheduling; Hydrogen energy storage system; Degradation cost; Weighed-MPC

1. Introduction

With the increasing pressure from energy consumption and environmental issues, both the penetration level and bulk injection of renewable energy have increased rapidly over the past decade [1]. As an emerging paradigm for renewable energy utilization, the integrated multi-energy microgrid is capable of coordinating the multi-forms of energy with respect to multi-dimensional supplies and demands [2]. However, relevant issues have come to light that

* Corresponding author.
E-mail address: jiayw@sustech.edu.cn (Y. Jia).

https://doi.org/10.1016/j.egyr.2021.08.037

Peer-review under responsibility of the scientific committee of the 4th International Conference on Electrical Engineering and Green Energy, CEEGE, 2021.

the stable operation of the multi-energy microgrid can be jeopardized by the inherent variability of the renewable energy outputs.

In practice, deploying an energy storage system is an effective solution to resolving the above-mentioned uncertain power fluctuation issues. On the one hand, relying on the ability of storing/releasing electricity energy, the energy storage systems can smooth the generation profile and facilitate secure operation states of the power systems. On the other hand, energy storage systems can be efficient to reduce the abandonment rate of wind and solar generation by converting and storing it into other forms of energy [3]. In general, for different energy storage technologies, the relevant cost, energy density, power density, responding time, and rated power of multiple units can be varied significantly. Therefore, it becomes highly interesting to investigate the economic benefit and mechanisms behind determining the appropriate energy storage technologies in a specific distributed system.

The hydrogen energy storage system (HESS) is currently attracting much attention with its high energy storage density and long lifetime [4]. According to the data reported by the Australian CSIRO, the HESS is more cost-competitive than most existing energy storage technologies e.g. battery energy storage [5]. For example, in some coastal areas, the impact of renewable energy fluctuations can be alleviated by deploying a seawater hydrogen production system, through which cost-efficient clean energy cycling can be achieved.

The multi-energy microgrid not only can integrate and manage the uncertainties from renewable energy but also can coordinate multiple forms of dispatchable energy in a holistic way, through which the system flexibility and energy utilization efficiency can thereby be improved. Toward this end, it is of vital importance to employ an effective energy scheduling strategy to globally manage such an integrated energy environment and instantly ensure the security and reliability of system operation.

1.1. Related work

In the literature, there are generally three classes of methods for energy scheduling in the concerned topic of this paper. The first class is the deterministic approach, where all the uncertainties are assumed to be fixed, and the decisions are made based on the forecasted or expected values of the uncertain factors. The second class of methods is non-deterministic approaches. In this class, uncertainties are represented by prediction intervals [6] or certain probability distributions [7]. The third class of methods is generally termed as online optimization approaches, which can adopt receding-horizon information within a shorter time scale (e.g. within 15 min–30 min) to achieve real-time energy scheduling [8,9].

In the integrated multi-energy microgrid, the heat–electricity cogeneration is of great economic and environmental benefits because of its high efficiency. In [10], the authors introduced the structure of a typical regional integrated multi-energy system, a summary of methods and problems related to the steady-state analysis of multi-energy systems is also provided. In [11], the authors proposed a general integrated multi-energy microgrid model including both the dynamic and static characteristics. In [12], the authors established a multi-energy complementary optimization scheduling model for an electricity–gas–heat system. The advantages of the power-to-gas operation in promoting wind power consumption and improving the system economy are illustrated in this work. In [13], an electric-heat hybrid model was studied, and the output characteristics and load side characteristics of renewable energy were analyzed. In [14], the elasticity of the electric-gas integrated energy system was improved by using the distributionally robust optimization model under extreme weather conditions. However, the integrated energy system is a complex system with multi-spatial scale and multi-time scale characteristics, and the interaction between systems is influenced by each other. How to optimize its operation reasonably is still one of the important problems.

Current multi-energy system researches rarely incorporate the HESS, whereas, in recent years, the HESS has been considered as a promising energy storage technology. Compared with lead–acid batteries and lithium-ion batteries, HESS is advantageous for its high energy storage density and long-life cycle, which make it especially suitable for large-scale energy storage. For the operation of HESS, it is necessary to analyze the cost of the degradation process. The degradation and remaining cycle life prediction are crucial for the hydrogen proton exchange membrane fuel cells (HPEMFCs) operation [15]. If the fuel cells (FCs) operate as a long-term storage system, cycling loads (low-power, high-power, transient-loading changes, and start/stop cycle) will be the main load demands, which will accelerate the degradation of the FCs [16]. Also, both running the FCs at high current densities for long periods and using the FCs to supply highly transient loads can negatively impact the performance of the FCs [17].

By surveying the state-of-the-art, it is found that a comprehensive model concerning multi-energy microgrid scheduling integrated with HESS and HSS considering three types of loads is rarely investigated. This hereby becomes the main focus of this paper.

1.2. Contributions

This paper comprehensively investigates a model of energy scheduling for a multi-energy microgrid with the integration of HESS and HSS. The main contributions of this paper are summarized as follows:

- A novel operation paradigm is proposed for microgrids embedded with HESS and HSS. The HESS with HPEMFCs can produce and sell the surplus hydrogen to the hydrogen refueling stations (HRSs) and make profits in case that the renewable energy is abundant, or convert the hydrogen back to electricity in case of deficiency of renewable generation.
- A hybrid model of energy scheduling is proposed for the integrated multi-energy microgrid, through which the day-ahead and real-time energy transactions can be optimally determined.
- The uncertainties induced by renewable energy generation, electrical load, hydrogen demand, and heat demand are explicitly modeled. To mitigate the impact of the uncertainties, we propose a novel flexible weighted Model Predictive Control (weighted-MPC) method, which can adjust the optimization time horizon adaptively according to the prediction accuracy for the uncertain factors.

The rest of this paper is organized as follows:

Section 2 describes the model of each component in the proposed integrated multi-energy microgrid. Section 3 describes the formulation of the proposed energy scheduling model. Section 4 analyzes the simulation results. Finally, we conclude our work in Section 5.

2. Preliminaries and model formulation

In this paper, a hybrid two-stage model for energy scheduling in HESS and HSS embedded multi-energy microgrid is proposed, where the different patterns between the electricity prices in the day-ahead market and the real-time market are properly considered. The fact is that the electricity purchased in the real-time market is more expensive than the one in the day-ahead market, and the electricity sold in the real-time market is cheaper than the one sold in the day-ahead market. Hence, the decision-making of energy transactions is concerned in the day-ahead market in our study. A grid-connected integrated multi-energy microgrid with HESS and HSS typically comprises five components including renewable generation units, system loads, the CHP units, the HESS, and the HSS. The overall configuration is shown in Fig. 1.

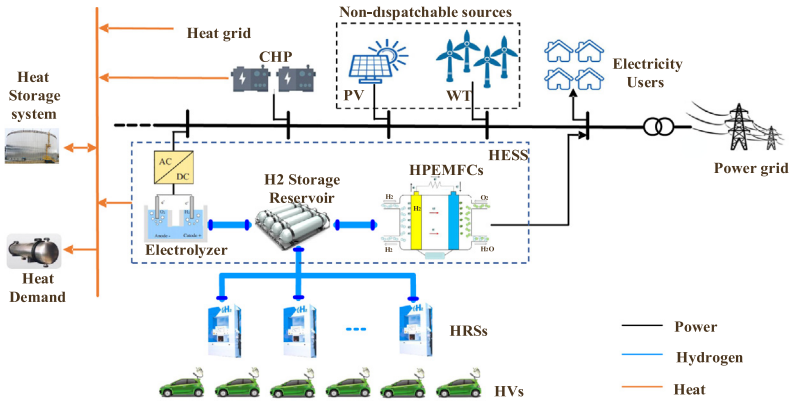

Fig. 1. The system model of grid-connected integrated multi-energy microgrid with HESS and HSS.

2.1. Renewable energy generation and system loads

In each time slot t, we denote the electrical load and renewable energy generation by $P_{e,t}$ and $P_{\text{renewable},t}$, respectively. We define net electrical load as follows:

$$P_{\text{load},t} = P_{e,t} - P_{\text{renewable},t} \tag{1}$$

In this paper, we define s_1, s_2 and s_3 denote the net electrical load, hydrogen demand, and heat demand scenarios, respectively. The hydrogen demand at time slot t is denoted as $D_{\mathrm{H}_2,t}$, and the heat demand at time slot t is denoted as h_t.

2.2. CHP units

In this paper, the CHP units are considered as the dispatchable generation units in the system. The fuel cost model for a CHP unit is shown in (2) and the start-up cost $c^{\mathrm{su}}_{\mathrm{G},i,t}$ is shown in (3):

$$C_{\mathrm{G},i,t} = a_{\mathrm{G},i} + b_{\mathrm{G},i} \cdot P_{\mathrm{G},i,t} + c_{\mathrm{G},i} \cdot \left(P_{\mathrm{G},i,t}\right)^2 \tag{2}$$

$$c^{\mathrm{su}}_{\mathrm{G},i,t} = d_{\mathrm{G},i} \left(y_{\mathrm{G},i,t} - y_{\mathrm{G},i,t-1}\right)^+ \tag{3}$$

where $y_{\mathrm{G},i,t}$ denotes the on/off status (1 = on, 0 = off); $P_{\mathrm{G},i,t}$ denotes the output power of the ith CHP unit; $a_{\mathrm{G},i}$, $b_{\mathrm{G},i}$, and $c_{\mathrm{G},i}$ represent the cost coefficients; $d_{\mathrm{G},i}$ denotes the start-up cost; $[\cdot]^+$ denotes a non-negative value.

In an integrated multi-energy microgrid, the CHP units are subject to the following operational constraints:

$$P^{\min}_{\mathrm{G},i} \le P_{\mathrm{G},i,t} \le P^{\max}_{\mathrm{G},i} \tag{4}$$

$$P_{\mathrm{G},i,t+1} - P_{\mathrm{G},i,t} \le R^{\mathrm{up}}_{G,i}, \;\; P_{\mathrm{G},i,t} - P_{\mathrm{G},i,t-1} \le R^{\mathrm{down}}_{\mathrm{G},i} \tag{5}$$

$$y_{\mathrm{G},i,\tau} \ge 1_{\{y_{G,i,t} > y_{G,i,t-1}\}}, t+1 \le \tau \le t + T^{\mathrm{on}}_i - 1 \tag{6}$$

$$y_{\mathrm{G},i,\tau} \le 1 - 1_{\{y_{G,i,t} < y_{G,i,t-1}\}}, t+1 \le \tau \le t + T^{\mathrm{off}}_i - 1 \tag{7}$$

where $P^{\min}_{\mathrm{G},i}$ and $P^{\max}_{\mathrm{G},i}$ denote the minimum and maximum power output of the ith CHP unit; $R^{\mathrm{up}}_{\mathrm{G},i}$ and $R^{\mathrm{down}}_{\mathrm{G},i}$ are the maximum upward and downward ramping rates of the ith CHP unit per time interval; $1_{\{\cdot\}}$ denotes the indicator function. Constraint (4) is the power output limits for the CHP units. Constraint (5) restricts the ramping limits. Constraints (6) and (7) are the minimum on/off time limits.

2.3. Hydrogen energy storage system operation model

2.3.1. HPEMFCs model

Hydrogen consumption of the HPEMFCs ($n_{\mathrm{H}_2,\mathrm{FC}}$) depends on its power output (P_{FC}) through the following relationship:

$$n_{\mathrm{H}_2,\mathrm{FC},t} = \frac{P_{\mathrm{FC},t}}{\eta_{\mathrm{FC}} LHV_{\mathrm{H}_2}} \tag{8}$$

$$m_{\mathrm{H}_2,\mathrm{FC},t} = n_{\mathrm{H}_2,\mathrm{FC},t} \cdot M_{\mathrm{H}_2} \tag{9}$$

where LHV_{H_2} is the lower value of hydrogen; M_{H_2} is the molar mass of hydrogen; η_{FC} is the efficiency of the HPEMFCs; $m_{\mathrm{H}_2,\mathrm{FC},t}$ is the mass of hydrogen consumption of the HPEMFCs at time slot t.

The degradation of the HPEMFCs will lead to a voltage drop. The start/stop cycle leads to the predominately comparable increase of fuel cell degradation. In our work, the relationship between power and voltage degradation is expressed by quadratic function through data fitting and expressed in (10):

$$\Omega_1(P_{\mathrm{FC},t}) = \alpha_1 \cdot P^2_{\mathrm{FC},t} + \beta_1 \cdot P_{\mathrm{FC},t} + \gamma_1 \tag{10}$$

where α_1, β_1 and γ_1 are coefficients of the HPEMFCs degradation function.

Based on the four operating conditions, the operational cost of HPEMFCs is therefore formulated as $C_{\mathrm{FC},t}$. $c^{\mathrm{su}}_{\mathrm{FC},t}$ and $c^{\mathrm{sd}}_{\mathrm{FC},t}$ are the start-up/shut-down cost of the HPEMFCs.

$$C_{\mathrm{FC},t} = \left(\frac{a_1}{N^{\mathrm{FC}}_{\mathrm{hours}}} + b_1\right) \cdot y_{\mathrm{FC},t} + c_1 \cdot \Omega_1(P_{\mathrm{FC},t}) \tag{11}$$

$$c^{\mathrm{su}}_{\mathrm{FC},t} = d_1 \cdot \left(y_{\mathrm{FC},t} - y_{\mathrm{FC},t-1}\right)^+, c^{\mathrm{sd}}_{\mathrm{FC},t} = e_1 \cdot \left(y_{\mathrm{FC},t-1} - y_{\mathrm{FC},t}\right)^+ \tag{12}$$

where a_1 and b_1 denote the fixed cost and the operation cost; $y_{\mathrm{FC},t}$ denotes the operational status (1 = on, 0 = off); $N^{\mathrm{FC}}_{\mathrm{hours}}$ denotes the service life; c_1 denotes the degradation cost coefficient; d_1 and e_1 denote the start-up and shut-down cost coefficients, respectively.

2.3.2. Electrolyzer (EL) model

Similar to the HPEMFCs model, the hydrogen molar flow of the electrolyzer ($n_{\mathrm{H_2,EL}}$) can be expressed as a function of the supplied electric power (P_{EL}):

$$n_{\mathrm{H_2,EL},t} = \frac{\eta_{\mathrm{EL}} P_{\mathrm{EL},t}}{LHV_{\mathrm{H_2}}} \tag{13}$$

$$m_{\mathrm{H_2,EL},t} = n_{\mathrm{H_2,EL},t} \cdot M_{\mathrm{H_2}} \tag{14}$$

where η_{EL} is the electrolyzer efficiency.

However, the degradation of the electrolyzer increases the cell voltage. In our work, we define the relationship between power and degradation of electrolyzer as the quadratic function which is similar to the HPEMFCs model. Thus, the cost of EL ($C_{\mathrm{EL},t}$, $c^{\mathrm{su}}_{\mathrm{EL},t}$, $c^{\mathrm{sd}}_{\mathrm{EL},t}$) can be easily formulated and will not be repeated here.

2.3.3. Hydrogen tank model

We use the level of hydrogen (LOH) to represent the state of the hydrogen tank, which is shown in (15):

$$LOH_t = LOH_{t-1} + \frac{\Re T_{\mathrm{H_2}}}{U_{\mathrm{H_2}}}(n_P - n_C) \tag{15}$$

where $\Re$ is the gas constant; $T_{\mathrm{H_2}}$ is the mean temperature inside the vessel; $U_{\mathrm{H_2}}$ is the overall tank volume; n_P and n_C denote the mass of hydrogen production and consumption, respectively.

The operational cost of the whole hydrogen energy storage system is shown in (16):

$$C_{\mathrm{HESS},t} = C_{\mathrm{FC},t} + C_{\mathrm{EL},t} \tag{16}$$

The HESS should subject to the following constraints.

$$m_{\mathrm{H_2,FC},t_k} + D_{\mathrm{H_2},t_k+1} \le \sum_{t=1}^{t_k-1}\left[m_{\mathrm{H_2,EL},t} - m_{\mathrm{H_2,FC},t}\right] - \sum_{t=2}^{t_k} D_{\mathrm{H_2},t} \tag{17}$$

$$0 \le y_{\mathrm{EL},t} + y_{\mathrm{FC},t} \le 1 \tag{18}$$

$$LOH^{\min} \le LOH_t \le LOH^{\max} \tag{19}$$

$$P^{\min}_{\mathrm{EL}} \le P_{\mathrm{EL},t} \le P^{\max}_{\mathrm{EL}},\ P^{\min}_{\mathrm{FC}} \le P_{\mathrm{FC},t} \le P^{\max}_{\mathrm{FC}} \tag{20}$$

$$LOH_1 = LOH_T \tag{21}$$

where $P^{\min}_{\mathrm{EL}}$, $P^{\max}_{\mathrm{EL}}$, $P^{\min}_{\mathrm{FC}}$ and $P^{\max}_{\mathrm{FC}}$ are the minimum and maximum power of EL and FCs, respectively. Constraint (17) limits the hydrogen consumption of HPEMFCs. Constraint (18) avoids the HPEMFCs and the EL working at the same time. Constraint (21) ensures that the value of LOH are equal at the beginning and the end of the scheduling horizon, which is beneficial to the circular scheduling of HESS.

2.4. Heat storage system model

In this paper, we combine the CHP system and hydrogen energy storage system with the heat storage system. Its mathematical model is as follows:

$$HS_t = (1 - \eta^{\mathrm{CHP}})HS_{t-1} + \delta_t \tag{22}$$

where HS_t denotes the heat storage power of the heat storage device at time t; η^{CHP} is the self-consumption rate of the heat storage device; δ_t is the storage/release heat level at time t.

For the whole heat storage system, the following constraints need to be met:

$$\eta_{\mathrm{G},i} \cdot \sum_{i=1}^{n} P_{\mathrm{G},i,t} + \eta_{\mathrm{HESS}} \cdot \left(P_{\mathrm{EL},t} + P_{\mathrm{FC},t}\right) + h_{\mathrm{EX},t} \ge \delta_t + h_t \tag{23}$$

$$0 \le h_{\mathrm{EX},t} \le h^{\max}_{\mathrm{EX}} \tag{24}$$

$$0 \le |\delta_t| \le \delta^{\max} \tag{25}$$

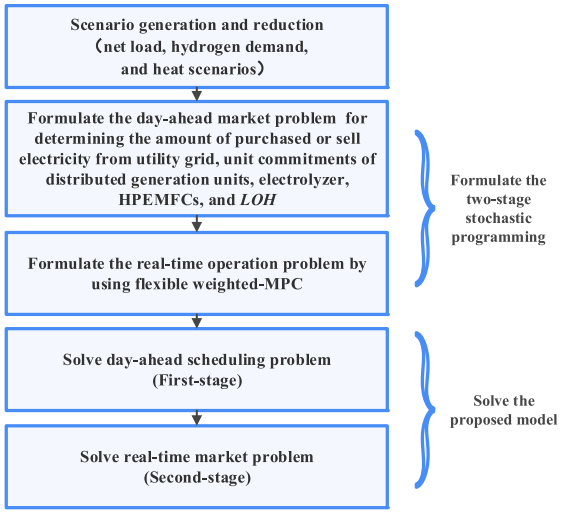

Fig. 2. The flowchart of solving process for the proposed model.

where $\eta_{G,i}$ is the heat recovery efficiency of the ith CHP unit; η_{HESS} is the heat recovery efficiency of the HESS; $h_{EX,t}$ is the heat level obtained externally; h_{EX}^{max} is the maximum value of buying heat externally; δ^{max} is the maximum value of the δ_t.

2.5. Other constraints

Since the concerned integrated multi-energy microgrid in our study operates in a grid-connected mode, so we can buy or sell the electricity based on the electricity price. Besides the above constraints, the following constraints also should be considered.

$$0 \le y_{buy,t}^{DA} \cdot P_{grid,t}^{DA,buy} + y_{buy,t}^{RT} \cdot P_{grid,t}^{RT,buy} \le P_{grid}^{max} \tag{26}$$

$$0 \le y_{sell,t}^{DA} \cdot P_{grid,t}^{DA,sell} + y_{sell,t}^{RT} \cdot P_{grid,t}^{RT,sell} \le P_{grid}^{max} \tag{27}$$

$$y_{buy,t}^{DA} + y_{sell,t}^{DA} \le 1, y_{buy,t}^{RT} + y_{sell,t}^{RT} \le 1 \tag{28}$$

where $y_{buy,t}^{DA}$, $y_{sell,t}^{DA}$, $y_{buy,t}^{RT}$, and $y_{sell,t}^{RT}$ denote the status of buy or sell electricity, respectively; $P_{grid,t}^{DA,buy}$, $P_{grid,t}^{DA,sell}$, $P_{buy,t}^{RT}$, and $P_{sell,t}^{RT}$ denote the power purchased from the utility grid and the power sold to the power grid, respectively. Constraint (28) prevents simultaneously buying and selling electricity.

3. Problem formulation

3.1. Two-stage scheduling model

The flowchart of solving process for the proposed model is shown in Fig. 2. In the first stage, the objective is to make an optimal decision on the unit commitments of distributed generation units, electrolyzer, HPEMFCs, and day-ahead energy transactions to minimize the operational cost. To better realize the circular scheduling of HESS, we require the value of *LOH* are equal at the beginning and the end of the scheduling horizon. Therefore, in the first stage, we also need to make decisions on LOH_t^{DA}. Here we neglect the network power loss and the production

cost of the renewable energy resources.

$$\begin{aligned}\min_{\left\{P^{\mathrm{DA,buy}}_{\mathrm{grid},t},P^{\mathrm{DA,sell}}_{\mathrm{grid},t},LOH^{\mathrm{DA}}_{t},y_{\mathrm{G},i,t},y_{\mathrm{FC},t},y_{\mathrm{EL},t}\right\}} C_{\mathrm{DA}} &= \sum_{t=1}^{T}\left(\lambda^{\mathrm{DA}}_{\mathrm{grid},t}\left[P^{\mathrm{DA,buy}}_{\mathrm{grid},t}-P^{\mathrm{DA,sell}}_{\mathrm{grid},t}\right]+c^{\mathrm{su}}_{\mathrm{G},i,t}\right.\\ &\left.+c^{\mathrm{su}}_{\mathrm{EL},t}+c^{\mathrm{su}}_{\mathrm{FC},t}+c^{\mathrm{sd}}_{\mathrm{EL},t}+c^{\mathrm{sd}}_{\mathrm{FC},t}\right)\\ &+\sum_{s_1}\sum_{s_2}\sum_{s_3} prob^{s_1}\cdot prob^{s_2}\cdot prob^{s_3}\\ &\cdot\sum_{t=1}^{T}\left[\begin{array}{l}\sum_{i=1}^{n}C^{s_1,s_2,s_3}_{\mathrm{G},i,t}+C^{s_1,s_2,s_3}_{HESS,t}+\lambda_{\mathrm{heat}}\cdot h^{s_1,s_2,s_3}_{\mathrm{EX},t}+\lambda^{\mathrm{RT,buy}}_{\mathrm{grid},t}\cdot P^{\mathrm{RT,buy},s_1,s_2,s_3}_{\mathrm{grid},t}\\ -\lambda^{\mathrm{RT,sell}}_{\mathrm{grid},t}\cdot P^{\mathrm{RT,sell},s_1,s_2,s_3}_{\mathrm{grid},t}+\lambda_p\cdot\left(LOH^{\mathrm{RT},s_1,s_2,s_3}_{t}-LOH^{\mathrm{DA}}_{t}\right)^2\end{array}\right]\end{aligned} \tag{29}$$

$$s.t.\ (4)\text{–}(7),\ (17)\text{–}(21),\ (23)\text{–}(28)$$

$$\sum_{i=1}^{n}P^{s_1,s_2,s_3}_{\mathrm{G},i,t}+P^{s_1,s_2,s_3}_{\mathrm{FC},t}+P^{\mathrm{DA,buy}}_{\mathrm{grid},t}+P^{\mathrm{RT,buy}}_{\mathrm{grid},t}\geq P_{\mathrm{load},t}+P^{s_1,s_2,s_3}_{\mathrm{EL},t}+P^{\mathrm{DA,sell},s_1,s_2,s_3}_{\mathrm{grid},t}+P^{\mathrm{RT,sell},s_1,s_2,s_3}_{\mathrm{grid},t} \tag{30}$$

where $\lambda^{\mathrm{DA}}_{\mathrm{grid},t}$, $\lambda^{\mathrm{RT,buy}}_{\mathrm{grid},t}$, and $\lambda^{\mathrm{RT,sell}}_{\mathrm{grid},t}$ are the day-ahead and real-time price, respectively; λ_{heat} is the price of buying heat externally; λ_p denotes the penalty cost. Constraint (30) is the power balancing constraint of the whole integrated multi-energy microgrid.

3.2. Flexible weighted-MPC model

In the second stage, we formulate the real-time operation problem in a weighted-MPC fashion [18]. In each period time t, the system operator minimizes the weighted total cost with a discount rate μ.

$$\min_{\left\{P_{\mathrm{G},i,t},P_{\mathrm{EL},t},P_{\mathrm{FC},t},h_{\mathrm{EX},t},P^{\mathrm{RT,buy}}_{\mathrm{grid},t},P^{\mathrm{RT,sell}}_{\mathrm{grid},t}\right\}}\ \sum_{t'=t}^{t'+H-1}\mu^{t'-t}C_{\mathrm{RT},t'} \tag{31}$$

$$C_{\mathrm{RT},t}=\sum_{i=1}^{n}C_{\mathrm{G},i,t}+C_{\mathrm{HESS},t}+\lambda_{\mathrm{heat}}\cdot h_{\mathrm{EX},t}+\lambda^{\mathrm{RT,buy}}_{\mathrm{grid},t}\cdot P^{\mathrm{RT,buy}}_{\mathrm{grid},t}-\lambda^{\mathrm{RT,sell}}_{\mathrm{grid},t}\cdot P^{\mathrm{RT,sell}}_{\mathrm{grid},t}+\lambda_p\cdot\left(LOH^{\mathrm{RT}}_{t}-LOH^{\mathrm{DA}}_{t}\right)^2 \tag{32}$$

Here, considering the optimization time horizon H can directly affect the optimization performance of the problem, we propose an adaptive algorithm to adjust H at the end of each rolling round. At the end of each flexible weighted-MPC rolling round, the optimization time horizon H should be updated by (33),

$$H^*=H-\psi \tag{33}$$

$$\psi=\begin{cases}4, & \varpi>2\\ 2, & 1<\varpi\leq 2\\ 0, & 0.6<\pi\leq 1\\ -2, & 0.3<\varpi\leq 0.6\\ -4, & 0\leq\varpi\leq 0.3\end{cases} \tag{34}$$

where ψ denotes the change of the optimization time horizon H; ϖ is the prediction accuracy of uncertain factors, which is the ratio of actual value to the difference value between the actual value and predicted value. This means when the prediction accuracy of uncertain factors is high, the optimization time horizon H increases, and vice versa.

3.3. Scenario reduction

In stochastic programming methods, the number of scenarios needed to accurately represent the uncertainties involved is usually very large, so scenario reduction methods are often used due to the complexity of calculation and time constraints. The goal is to select those scenarios that can approximate the potential probability distribution well without losing important information. There are two types of scenario reduction methods, namely forward selection and backward reduction [19]. However, compared with the forward selection, the backward reduction is easier to ignore the small probability events in some extreme cases.

In this paper, we used a developed backward reduction algorithm based on [19]. The developed backward reduction algorithm is presented in Fig. 3.

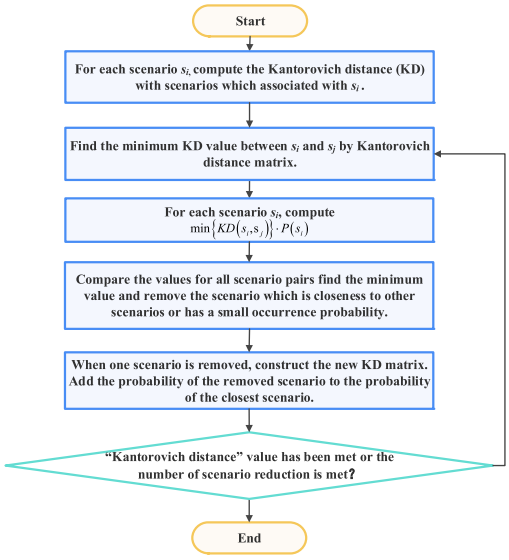

Fig. 3. The flowchart of the developed backward reduction algorithm.

4. Case study

Numerical experiments are conducted in MATLAB with YALMIP [20] on the computing platform with Intel(R) Core(TM) i7-7700 CPU.

4.1. Case configuration

Table 1 provides the parameters of the two CHP units. Table 2 provides the parameters of the HESS. In this paper, we assume that the day-ahead and real-time electricity prices over 24 h can be accurately predicted, as presented in Table 3. The prediction error in the day-ahead stage is very large, and can even reach more than 30%. In this work, we use the Monte Carlo method for simulation scenario generation based on real renewables generation and load data and assume the forecasting errors follow a normal distribution. Each uncertainty variable (net electricity load, hydrogen demand, and heat demand) has fifty scenarios, which is shown in Fig. 4. Each uncertainty variable has 10 scenarios by the backward scenario reduction method.

4.2. Performance evaluation

To illustrate the influence of FCs on the system operation, we solve the energy scheduling problem of the integrated multi-energy microgrid model with FCs and without FCs, respectively. The operational results for the integrated multi-energy microgrid with FCs and without FCs are illustrated in Figs. 5–8. Fig. 5 shows the transaction

Table 1. Parameter settings for scheduling generators.

	$P^{\max}$ (kW)	$P^{\min}$ (kW)	$a_{G,i}$ ($)	$b_{G,i}$ ($/kWh)	$c_{G,i}$ ($)	R^{up} (kW/min)	R^{down} (kW/min)	T^{on}/T^{off} (h)
G1	100	20	0.57	0.12	0.056	40	30	1/1
G2	80	10	0.41	0.15	0.04	30	20	1/1

Table 2. Parameter settings for HESS.

	a ($/kW)	b ($/h)	c ($)	d ($)	N_{hours} (h)	η
EL	9.2845	0.00226	0.11	0.005648	30 000	0.72
FC	33.885	0.00113	0.11	0.005648	30 000	0.6

Table 3. Electricity spot price in one day.

Time period (h)	$[0, 6] \cup [22, 24]$	$[7, 10] \cup [18, 22]$	$[11, 17]$
λ_{grid}^{DA}	0.2326	0.6860	0.4593
$\lambda_{grid}^{RT,buy}$	0.3024	0.8918	0.5971
$\lambda_{grid}^{RT,sell}$	0.1628	0.4802	0.3215

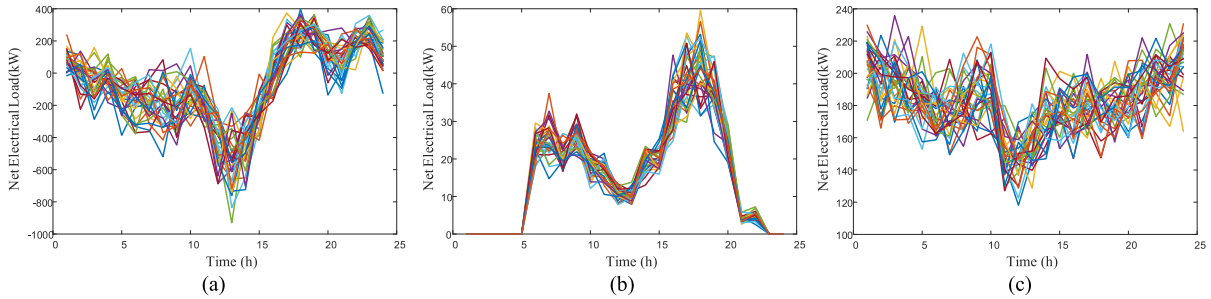

Fig. 4. Scenarios of net electrical load, hydrogen demand and heat demand over 24 h, (a) the net electrical load; (b) the hydrogen demand; (c) the heat demand.

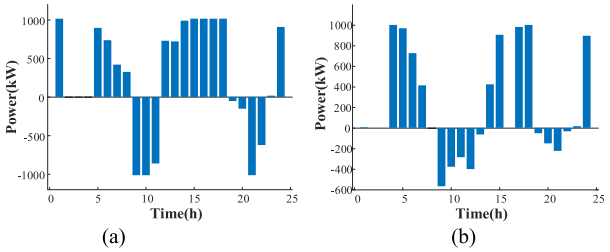

Fig. 5. The power from power grid: (a) with FCs; (b) without FCs.

power with the power grid, which helps the multi-energy microgrid system maintain the power balance. The power of EL/FCs is shown in Fig. 6. Fig. 7 presents the *LOH* of the HESS over 24 h. Because the grid electricity price is cheaper in the early morning and the wind power output oversupplies demand, the HESS starts to convert electricity to hydrogen as much as possible. When the grid electricity price and electrical load increase, the HESS begins to return the stored hydrogen to the FCs and convert hydrogen to electricity at peak demand time which can be seen in Fig. 6. The heat level obtained externally is shown in Fig. 8. The use of hydrogen fuel cells reduces the cost of heat acquisition by reducing the amount of heat from the outside.

To compare the performance of the deterministic approach and the stochastic approach, we use the same set of actual profiles including net electricity load, hydrogen demand, and heat demand to simulate the real-time

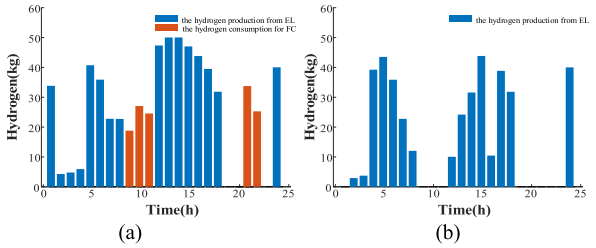

Fig. 6. The hydrogen production from EL and consumption by FCs: (a) with FCs; (b) without FCs.

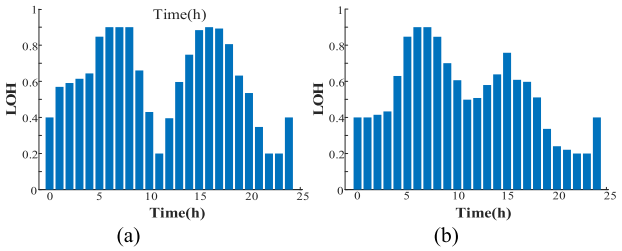

Fig. 7. The level of hydrogen in the hydrogen energy storage system: (a) with FCs; (b) without FCs.

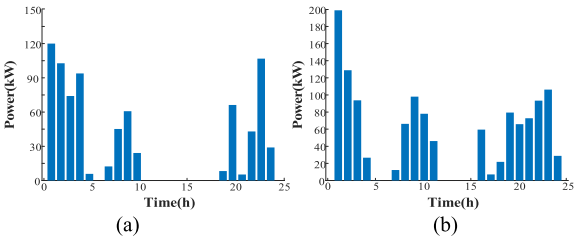

Fig. 8. The heat level obtained externally: (a) with FCs; (b) without FCs.

operation in the case study. Firstly, we run the deterministic approach and the stochastic approach to obtain day-ahead solutions, respectively. We then fix the number of energy transactions in the day-ahead market, replace the forecasts with the real net electrical load, hydrogen demand, and heat demand, and run the deterministic approach again. To compare the performance of the integrated multi-energy microgrid energy scheduling, we perform both the stochastic approach and deterministic approach for half a month. And the deterministic approach is based on the predicted information. Fig. 9 shows the daily operational cost deviation between both the stochastic approach and deterministic approach and perfect dispatch over half a month under. The stochastic approach outperforms the deterministic approach in terms of the operational cost.

Fig. 10 presents the cost of the integrated multi-energy microgrid with FCs and without FCs over several days. It can be observed that the use of FCs can effectively reduce costs because FCs can convert hydrogen to electricity at peak demand time, especially at high tariff periods. It can be concluded that the hydrogen energy storage system with FCs can convert hydrogen to electricity when renewable energy generation is insufficient and the integrated multi-energy microgrid with FCs can make better use of the surplus renewable energy and increase the reward of the system by realizing the electricity–hydrogen–electricity conversion.

5. Conclusion

Hydrogen energy storage system, which can realize the electricity–hydrogen–electricity conversion, has emerged to become an alternative solution to handling system uncertainties and increasing energy utilization efficiency. In this paper, a hybrid model for energy scheduling for HESS and HSS embedded microgrid is proposed to take advantage of the local distributed energy resources and efficiently meet multi-dimensional demands through a

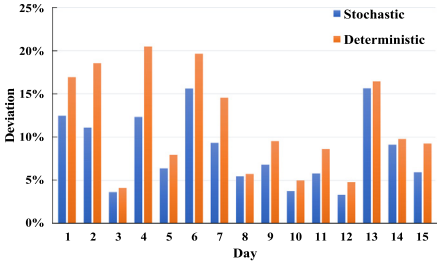

Fig. 9. The daily operational cost of the integrated multi-energy microgrid over half a month.

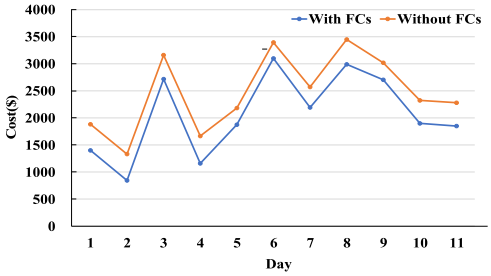

Fig. 10. The daily operational cost of the integrated multi-energy microgrid with FCs and without FCs.

complete hydrogen generation-consumption cycling. Distinguished from the existing framework, our model suggests a high potential that the hydrogen can be transported to the HRSs or converted into electricity by hydrogen FCs. Simulation results show that the hybrid two-stage model in this paper can reduce the impact of load uncertainty to a certain extent and improve the economy of the system operation. As compared to the case without FCs, the one with FCs provide better performance in scheduling the distributed resources.

Declaration of competing interest

The authors declare that they have no known competing financial interests or personal relationships that could have appeared to influence the work reported in this paper.

Acknowledgments

This work was supported in part by Natural Science Foundation of China (72071100), Guangdong Basic and Applied Basic Research Fund, China (2019A1515111173, 2019A1515110901), Young Talent Program (Dept. of Education of Guangdong Province, China) (2018KQNCX223), and High-level University Fund, China (G02236002).

References

[1] Lyu Xue, Jia Youwei, Xu Zhao. A novel control strategy for wind farm active power regulation considering wake interaction. IEEE Trans Sustain Energy 2019;11(2):618–28.
[2] Yun Jingyang, Yan Zheng, Yun Zhou, Zhang Peichao, Weidong Hu. Multi-time collaborative restoration for integrated electrical-gas distribution system based on rolling optimization. CSEE J Power Energy Syst 2020. http://dx.doi.org/10.17775/CSEEJPES.2020.03720.
[3] Zhu Mengting, Xu Chengsi, Dong Shufeng, Tang Kunjie, Gu Chenghong. An integrated multi-energy flow calculation method for electricity-gas-thermal integrated energy systems. Prot Control Mod Power Syst 2021;6(1):65–76.
[4] Xu Bolun, et al. Modeling of lithium-ion battery degradation for cell life assessment. IEEE Trans Smart Grid 2016;9(2):1131–40.
[5] CSIRO Roadmap finds hydrogen industry set for scale-up. 2021, [Online]. Available: https://www.csiro.au/en/News/News-releases/2018/Roadmap-finds-Hydrogen-Industry-set-for-scale-up (Accessed on May 30, 2021).
[6] Alvaro Lorca, Sun Xu Andy. Adaptive robust optimization with dynamic uncertainty sets for multi-period economic dispatch under significant wind. IEEE Trans Power Syst 2015;30(4):1702–13.
[7] Gu Yingzhong, Xie Le. Stochastic look-ahead economic dispatch with variable generation resources. IEEE Trans Power Syst 2016;32(1):17–29.

[8] Jia Youwei, et al. A novel retrospect-inspired regime for microgrid real-time energy scheduling with heterogeneous sources. IEEE Trans Smart Grid 2020;11(6):4614–25.
[9] Jia Youwei, et al. A retroactive approach to microgrid real-time scheduling in quest of perfect dispatch solution. J Mod Power Syst Clean Energy 2019;7(6):1608–18.
[10] Wang Weiliang, et al. Review of steady-state analysis of typical regional integrated energy system under the background of energy internet (in Chinese). Proc CSEE 2016;36:3292–305.
[11] Tian Liting, et al. System modeling and optimal dispatching of multi-energy microgrid with energy storage. J Mod Power Syst Clean Energy 2020;8(5):809–19.
[12] Wei Zhenbo, et al. Joint economic scheduling of power-to-gas and thermoelectric decoupling CHP in regional energy internet. Power Syst Technol 2018;42(11):3512–20.
[13] Henning Hans-Martin, Palzer Andreas. A comprehensive model for the german electricity and heat sector in a future energy system with a dominant contribution from renewable energy technologies—Part I: Methodology. Renew Sustain Energy Rev 2014;30:1003–18.
[14] Zhang Yachao, et al. Prevention strategy for elastic improvement of an electricity-gas integrated energy system based on optimization of sub-brochure rods (in Chinese). Autom Electr Power Syst 2021.
[15] Li Jianqiu, et al. Fuel cell system degradation analysis of a Chinese plug-in hybrid fuel cell city bus. Int J Hydrogen Energy 2016;41(34):15295–310.
[16] Pei Pucheng, Chen Huicui. Main factors affecting the lifetime of proton exchange membrane fuel cells in vehicle applications: A review. Appl Energy 2014;125:60–75.
[17] Fletcher Tom, Thring Rob, Watkinson Martin. An energy management strategy to concurrently optimise fuel consumption & PEM fuel cell lifetime in a hybrid vehicle. Int J Hydrogen Energy 2016;41(46):21503–15.
[18] Lyu Cheng, et al. Real-time operation optimization of islanded microgrid with battery energy storage system. In: 2020 ieee power & energy society general meeting (pesgm). IEEE; 2020.
[19] Razali, Muhamad NM, Hashim AH. Backward reduction application for minimizing wind power scenarios in stochastic programming. In: 2010 4th international power engineering and optimization conference (peoco). IEEE; 2010.
[20] Lofberg Johan. YALMIP: A toolbox for modeling and optimization in MATLAB. In: 2004 ieee international conference on robotics and automation (ieee cat. no. 04ch37508). IEEE; 2004.